Front. Environ. Sci. Eng. 2018, 12(4): 11
https://doi.org/10.1007/s11783-018-1072-5

RESEARCH ARTICLE

# Algal biomass derived biochar anode for efficient extracellular electron uptake from *Shewanella oneidensis* MR-1

**Yan-Shan Wang[1], Dao-Bo Li[1], Feng Zhang[1], Zhong-Hua Tong (✉)[1,2], Han-Qing Yu[1]**

1 CAS Key Laboratory of Urban Pollutant Conversion, Department of Applied Chemistry, University of Science & Technology of China, Hefei 230026, China

2 Anhui Province Key Laboratory of Polar Environment and Global Change, University of Science & Technology of China, Hefei 230026, China*

## HIGHLIGHTS

- Algal biochar anode produced higher biocurrent compared with graphite plate anode.
- Algal biochar exhibited stronger electrochemical response to redox mediators.
- Algal biochar showed excellent adsorption to redox mediators.

## GRAPHIC ABSTRACT

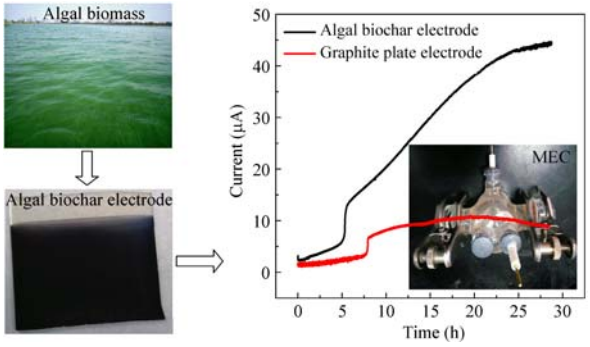


## ARTICLE INFO

*Article history:*
Received 5 April 2018
Revised 6 July 2018
Accepted 6 July 2018
Available online 4 August 2018

*Keywords:*
Algal biochar
Anode material
Electrochemical activity
Extracellular electron transport
Waste resource utilization

## ABSTRACT

The development of cost-effective and highly efficient anode materials for extracellular electron uptake is important to improve the electricity generation of bioelectrochemical systems. An effective approach to mitigate harmful algal bloom (HAB) is mechanical harvesting of algal biomass, thus subsequent processing for the collected algal biomass is desired. In this study, a low-cost biochar derived from algal biomass via pyrolysis was utilized as an anode material for efficient electron uptake. Electrochemical properties of the algal biochar and graphite plate electrodes were characterized in a bioelectrochemical system (BES). Compared with graphite plate electrode, the algal biochar electrode could effectively utilize both indirect and direct electron transfer pathways for current production, and showed stronger electrochemical response and better adsorption of redox mediators. The maximum current density of algal biochar anode was about 4.1 times higher than graphite plate anode in BES. This work provides an application potential for collected HAB to develop a cost-effective anode material for efficient extracellular electron uptake in BES and to achieve waste resource utilization.



## 1 Introduction

Bioelectrochemical systems (BESs), such as microbial electrolysis cells (MECs) and microbial fuel cells (MFCs), possess tremendous potential for biosensors, sewage treatment and renewable energy generation (Koposova et al., 2014; Xiao et al., 2016; Mohanakrishna et al., 2018) due to their moderate operational conditions and wide range of organic substrates. Anodic process, that utilizes bacteria as a catalyst to directly convert organic matter into electrons, protons and $CO_2$, plays an important role in BESs. The electrons will go through external circuit to generate electricity, and the protons will travel through the solution to produce water (Zhang and Angelidaki, 2014). However, one of the bottlenecks for BES application is the

✉ Corresponding author
E-mail: zhtong@ustc.edu.cn

*Special Issue—Bio-based Technologies for Resource Recovery (Responsible Editors: Aijie Wang & David Stuckey)

low output power. Promoting extracellular electron transfer (EET) from bacteria to anode is very important to improve the performance of BES. Anodic efficiency can be improved by isolating electrochemically active bacteria (Xing et al., 2010; Sacco et al., 2017) and developing new anode materials (Bian et al., 2018; Chen et al., 2018a; 2018b).

Three unique electron transport pathways have been proposed, including indirect electron transport through mediators, direct electron transport via c-type cytochromes, and electron transport through conductive nanowires between electrode and bacteria (Liu et al., 2010; Alshehri, 2017). Direct electron transfer is thought to be the dominant EET pathway (Ma et al., 2016; Bian et al., 2018). Over the past several years, studies on developing anode materials for efficient extracellular electron uptake focused mainly on direct electron transfer through cell surface proteins, where the formation of biofilm on the electrode is important. Zhang et al. (2015) have reported a distinct study that sustained electron transfer in BESs was obtained using $WO_3$ nanorods-modified carbon electrode with suppressed biofilm formation, which suggests indirect EET is important under this situation. Kotloski and Gralnick (2013) demonstrated flavin electron shuttling contributed to approximately 75% of extracellular electron transfer and dominated EET by *Shewanella oneidensis*, implying that the interaction between electrode and mediators also plays an important role in the EET process. Therefore, it would be promising for extracellular electron transfer if the anode material had both strong electrochemical response to redox mediators and great biological compatibility for bacterial localization.

Harmful algal blooms (HABs) occur frequently worldwide in eutrophic lakes and reservoirs (Guo, 2007) and induce undesired taste and odor, severely threatening aquatic life and human health (MacKintosh et al., 1990; Su et al., 2016). In China, large-scale mechanical harvesting of algal biomass has been widely applied to alleviate HABs in recent years (Guo, 2007). Further processing of the collected algal biomass is needed. Biochar is a carbon-rich solid material made from biomass via pyrolysis. It has been applied for many aspects, such as adsorption, carbon dioxide capture, and soil amendment (Chan et al., 2008; Liu et al., 2013; Creamer et al., 2014). Biochar production from freshwater algae by pyrolysis has been previously reported (Meng et al., 2015; Roberts et al., 2015; Zheng et al., 2017). Some studies have shown that biochar had great biological compatibility in promoting interspecies electron transfer and colonization of functional microbes (Chen et al., 2014; Luo et al., 2015). Therefore, we propose algal-bloom derived biochar can be used as an anode material for effective electron uptake and to achieve waste resource utilization.

In this work, the low-cost biochar derived from algal bloom was used as an anode material for efficient extracellular electron uptake in BESs with *S. oneidensis* MR-1 as a model electricity production strain. Our results show that the biochar-derived anode could effectively utilize both direct and mediated electron transfer pathways. Compared with graphite plate electrode, the biochar anode demonstrated stronger electrochemical response and better adsorption of redox mediator. Analysis of current generation curves showed that algal biochar electrode had greater electricity generation ability in BESs. Potential mechanisms for improved electrochemical activity were discussed.

## 2 Materials and methods

### 2.1 Algal biochar

Algal biomass was collected in August 2015 from an algae water separation station on Lake Chaohu, Hefei, China. The algal biomass was dried at 105°C and ground in an agate mortar before passing through a 100 mesh sieve. After mixing 5 g of the resulting algal biomass with KOH at a mass ratio of 1:1, the mixture was pyrolyzed in an argon-protected tube furnace at 750°C for 3 h with a temperature ramp of 10°C/min. Then 5% HCl and distilled water were used sequentially to clean up. The obtained samples were dried using a vacuum oven at 60°C and ground to obtain biochar as described by Xiong et al. (2015).

### 2.2 Fabrication of electrodes

Algal biochar electrode was fabricated by electrophoresis deposition to deposit algal biochar onto the surface of clean ITO glass substrate. Five mg of the biochar and 20 mg of iodine were added to 100 mL of acetone and mixed using sonication for 30 min. The suspension was added into a beaker with two ITO glasses kept about 1 cm apart and electrophoresed at 12 V for 5 min. The ITO glass with biochar deposited was then taken out for acetone evaporation, followed by heating at 200°C in an oven for 2 h to remove iodine, and finally algal biochar electrode was obtained. Before use, commercial graphite plate electrodes (30 mm × 30 mm; 2 mm thickness) were polished using aluminum oxide sandpaper (1200 #), and washed with distilled water and dried at 105°C.

Scanning electron microscope (SEM) was used to observe the surface morphology of the algal biochar and graphite plate electrodes before and after BES operation. The algal biochar and graphite plate electrodes after BES operation were pretreated as described by Zhang et al. (2015). Functional groups of the biochar were identified using Nicolet 8700 FT-IR spectrometer with the KBr disk method. Raman spectra of the biochar were recorded with a LabRamHR spectrometer (HORIBA Jobin Yvon,

France) at 514 nm. The surface area was determined by the BET method with a Builder 4200 instrument (Tristar II 3020M, Micromeritics Co., USA) at liquid nitrogen temperature.

### 2.3 Bacteria strain and culture conditions

A frozen stock of *S. oneidensis* MR-1 was inoculated into LB medium and grown aerobically at 30°C overnight. The bacteria solution was added into a mineral medium (20 mmol/L lactate as the electron donor) at a volume ratio of 1:1000 and grown for 24 h with shaking at 200 r/min. The culture was then inoculated to a mineral medium (20 mmol/L lactate and 40 mmol/L fumarate as the electron donor and acceptor, respectively) at a volume ratio of 1:10. After anaerobically growing for about 8 h, 100 mL of the culture was added into anode chamber with 20 mmol/L lactate as the substrate for electricity generation. The mineral medium composition was described previously (Li et al., 2017) but vitamins or amino acids were eliminated. HEPES was added at 30 mmol/L to buffer against pH change. The pH of the medium was adjusted to about 7.0 and then autoclaved. To prepare anaerobic mineral medium, oxygen in the medium was removed under $N_2$ sparging for about 20 min before autoclaving.

### 2.4 BES construction and operation

Single chamber membrane-free BES with three-electrode system was used in this study. The anodic chamber had a volume of about 120 mL. A Pt wire as the counter electrode and an Ag/AgCl (KCl sat.) as the reference electrode were used. The algal biochar electrode was employed as the anode and graphite plate electrode was used in the control experiment. The anode was set at a constant potential (0.2 V vs. Ag/AgCl). The experiments were done at 30°C.

### 2.5 Electrochemical analysis

Currents were recorded using a multichannel potentiostat (CHI 1030C, Chenhua Instrument Co., Shanghai, China) every 3 s. Cyclic voltammetry (CV) curves in BESs were obtained when the current reached the maximum level. The CV scanning was conducted at a rate of 2 mV/s with a potential range from –0.8 V to 0.25 V vs. Ag/AgCl followed by a reverse scan. For electrochemical impedance spectroscopy (EIS), an open circuit potential was utilized as an initial potential. EIS measurements were carried out in 10 mmol/L $[Fe(CN)_6]^{3-/4-}$ with 0.1 mol/L KCl for sterile electrode or bioanode from 0.1 Hz to 100 kHz with 5 mV amplitude under open-circuit potential conditions. ZView 2 software (Scribner and Associates, USA) was used to fit the EIS data to equivalent circuit. Three-electrode systems were used for all the electrochemical measurements as described above.

## 3 Results and discussion

### 3.1 Physicochemical property of electrodes

The dimension and surface morphology of algal bloom derived biochar electrode and graphite plate electrode were determined by SEM analysis. The biochar particles on the electrode surface have diverse sizes, ranging from ca. 100 nm to 3 μm (Fig. 1(a)). Compared with graphite plate electrode, algal biochar electrode had higher surface roughness (Figs. 1(a) and 1(b)) which could favor bacteria adhesion as demonstrated by Zhang et al. (2011). FTIR and Raman techniques were applied to further characterize the chemical properties of the prepared electrodes. As shown in Fig. 1(c), the FTIR spectrum of the algal biochar displays four obvious absorption peaks at 470, 1093, 1625 and 3448 $cm^{-1}$, respectively. The peak at 470 $cm^{-1}$ can be assigned to Si-O bending (Bertaux et al., 1998). The peak around 1093 $cm^{-1}$ was caused by C-N stretching vibration (Lv et al., 2003). The peak at 1625 $cm^{-1}$ can be attributed to aromatic C = C vibrations, while the peak at 3448 $cm^{-1}$ corresponds to O-H stretching from alcohol, phenols and carboxylic acids (Suguihiro et al., 2013). For graphite plate, two weak absorption peaks at 1632 and 3435 $cm^{-1}$ were observed, corresponding to the characteristic absorbance of C = C vibrations and O-H stretching, respectively (Fig. 1(c)). These results indicate that the algal biochar anode has more oxygen-containing functional groups. Previous studies have shown that cytochromes can be attached to carboxylic acid terminus by forming strong hydrogen bonding (El Kasmi et al., 1998; Avila et al., 2000), suggesting oxygen-containing functional groups might enhance direct electron transfer by facilitating the interaction between bacteria and electrode (Zhang et al., 2016; Wu et al., 2017).

Amorphous and graphite phases of carbon can be identified by Raman spectra (Ferrari and Robertson, 2000). Figure 1(d) shows the Raman spectra of the electrode materials. The peak at a wavenumber around 1322 $cm^{-1}$ can be assigned to the amorphous carbon (D band), and that of 1599 $cm^{-1}$ is a characteristic of the graphite phase (G band). The graphitic degree of carbon materials can be reflected by the intensity ratio of D and G bands. Compared with the graphite plate electrode with $I_D/I_G$ ratio of 0.54, the algal biochar electrode has higher $I_D/I_G$ value of 1.35, suggesting that the surface of algal biochar electrode possesses more defects and lower graphitized degree. Previous study reported that graphite plate anode with higher graphitized degree had relatively low bacteria attachment (ter Heijne et al., 2008), suggesting the algal biochar electrode is good for biofilm formation.

### 3.2 Enhanced electricity generation in BES

The ability to generate electricity is a significant parameter for evaluation of anode material. Graphite materials are

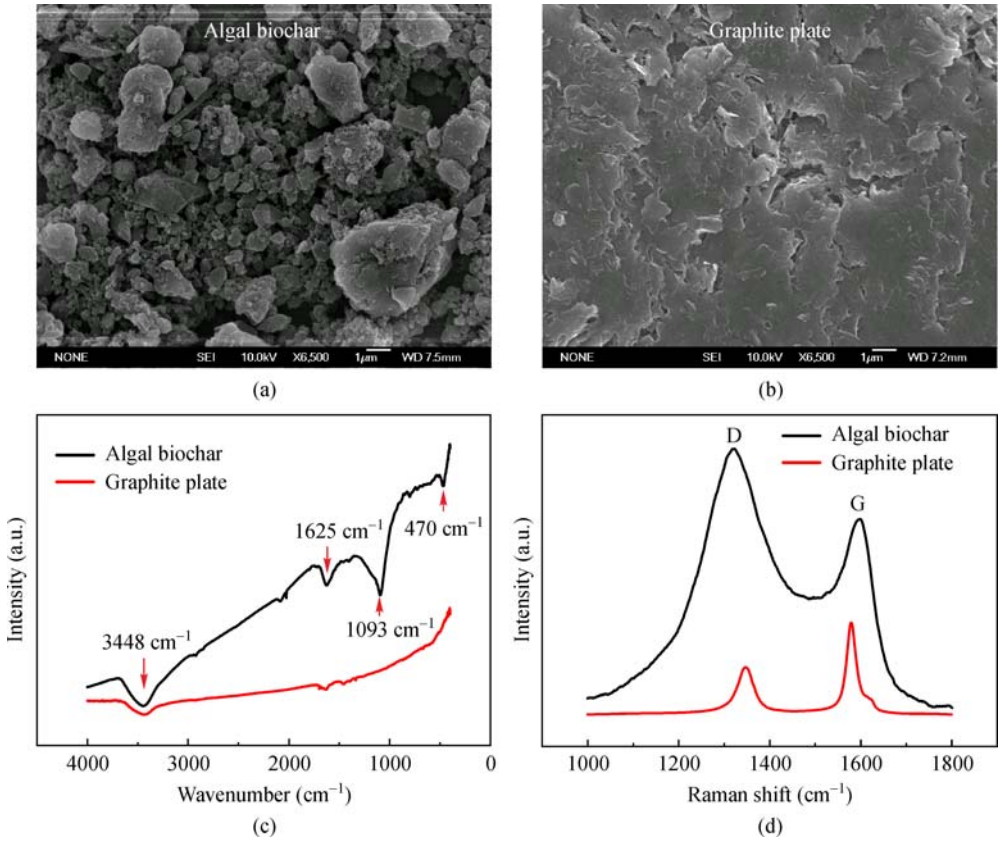


**Fig. 1** Characterization of algal biochar and graphite plate electrodes. (a) and (b) SEM images; (c) FT-IR spectra; (d) Raman spectra

commonly used as electrodes in BESs. ter Heijne et al. (2008) have demonstrated the good biocurrent generation ability of graphite plate anode. Therefore, the ability of algal biochar anode to generate electricity in BES was studied and compared with that of graphite plate anode. Figure 2 shows the process of electricity output in BESs with algal biochar and graphite plate anodes. When the bacteria cells were injected into electrolytic chambers, currents were generated soon. After 5 h, the current began an exponential increase in the BES with biochar anode and reached its maximum level of ca. 44.6 μA in 28 h. The current generation with graphite anode had an abrupt increase from 4 to 6.5 μA at 8 h and then gradually increased to its highest level of 10.8 μA in 20 h. The algal biochar anode produced a maximum current density of about 9.1 μA/cm$^2$, which was approximately 4.1 times higher than that of the graphite plate anode (2.2 μA/cm$^2$). Moreover, electricity generation by algal biochar electrode is higher than that produced by some carbon materials, such as graphite disk and carbon paper (Table 1). Although Au modified anode showed better performance, Au is an expensive noble metal. The good performance of 3D carbon may be ascribed to its 3D porous structure. In addition, the electricity generation by algal biochar anode (9.1 μA/cm$^2$) was comparable to porous carbon paper anode (8.5 μA/cm$^2$) (Kim et al., 2005). These results

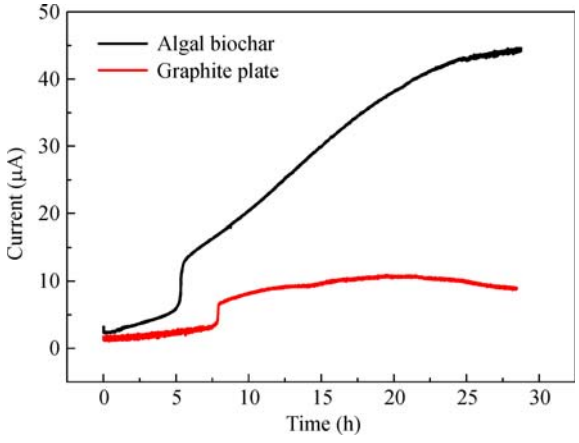


**Fig. 2** Time course of current output with different electrodes in BESs

indicate that algal bloom derived biochar is an effective anode material for extracellular electron uptake in BESs.

### 3.3 Extracellular electron transfer (EET) mechanism

To understand the performance of the algal biochar electrode, EET mechanisms were analyzed using different methods. EIS is a powerful nondestructive technique to

**Table 1** Comparison of the maximum current density of different anode materials

| Anode materials | Anode microbe | $I_{max}$ (μA/cm$^2$) | Reference |
|---|---|---|---|
| Graphite disk | *S. oneidensis* MR-1 | 3.6 | Fan et al. (2011) |
| Graphite/Au | *S. oneidensis* MR-1 | 74.4 | Fan et al. (2011) |
| Graphite/Pd | *S. oneidensis* MR-1 | 8.8 | Fan et al. (2011) |
| Carbon paper | *S. oneidensis* MR-1 | ~3.8 | Zhang et al. (2015) |
| Carbon paper/$WO_3$ | *S. oneidensis* MR-1 | ~ 4 | Zhang et al. (2015) |
| 3D porous carbon | *S. oneidensis* MR-1 | ~38.2 | Bian et al. (2018) |
| Porous carbon paper | Anaerobic sewage sludge | ~8.5 | Kim et al. (2005) |
| Graphite plate | *S. oneidensis* MR-1 | 2.2 | This study |
| Algal biochar | *S. oneidensis* MR-1 | 9.1 | This study |

identify the circuit elements (Kashyap et al., 2014). We performed EIS for the two sterile electrodes. As shown in Fig. 3(a), EIS curve of the sterile algal biochar electrode shows a semicircle with lager diameter than that of sterile graphite plate electrode, implying the sterile graphite plate electrode possess lower the electron transfer resistance than the sterile algal biochar electrode. By fitting the EIS spectra to an equivalent circuit, the values of ohmic resistance ($R_s$) and charge transfer resistance ($R_{ct}$) were determined (Fig. 3(b)). The $R_s$, indicating the intrinsic electrical conductivity of electrodes, and $R_{ct}$ at the electrode/electrolyte interface are important parameters for assessing the catalytic activity of electrodes. The $R_s$ of sterile algal biochar electrode is 3.8 Ω, much higher than 1.1 Ω for the sterile graphite plate electrode, indicating that the conductivity of sterile algal biochar electrode was lower than that of sterile graphite plate electrode. The $R_{ct}$ of sterile algal biochar electrode was 1.3 times higher than that of sterile graphite plate electrode, further suggesting faster charge transfer on the surface of sterile graphite plate

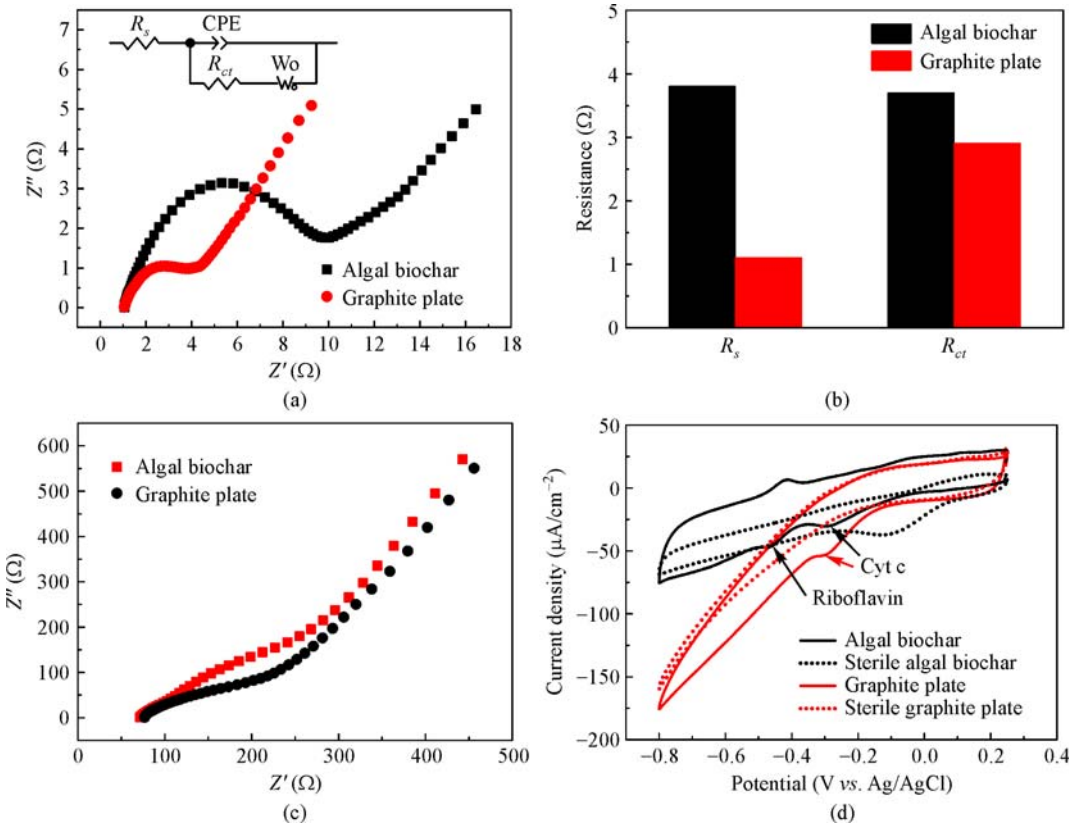


**Fig. 3** (a) Electrochemical impedance spectra of sterile electrodes in 10 mmol/L $[Fe(CN)_6]^{3-/4-}$ with 0.1 mol/L KCl; (b) Ohmic resistance ($R_s$) and charge transfer resistance ($R_{ct}$) of the sterile electrodes; (c) Electrochemical impedance spectra of graphite plate and algal biochar electrodes in BES; (d) The CV profiles of sterile electrodes and the electrodes in BESs

electrode. However, the BES with algal biochar electrode demonstrated greater performance in current generation than graphite electrode. These results suggest that some mechanisms may contribute to the greater biocurrent generation in the BES with algal biochar anode. We further performed EIS for the electrodes in BESs when the current reach their maximum levels. As shown in Fig. 3(c), the EIS curve of algal biochar electrode shows a semicircle with smaller diameter than that of graphite plate electrode. The result indicated that algal biochar anode had lower resistance than graphite plate anode in BESs, which could be a result of more bacteria attachment on the biochar anode as shown in the SEM images (Fig. 4). The interaction between MR-1 cells and the algal biochar electrode may improve the performance.

Redox reactions involved in EET to the anode of BESs can be identified using cyclic voltammetry (CV). CV assessment with a low scan rate of 2 mV/s was performed to investigate the potential mechanisms for enhancing current generation. As shown in Fig. 3(d), CV profile of the graphite anode showed a reduction peak at –200 mV which could be attributed to direct electron transfer of cytochromes (Wang et al., 2017), while no obvious peak corresponding to flavins was observed, suggesting direct electron transfer was an effective process using graphite anode for electricity production. In algal biochar anode system, two cathodic peaks located at about –299 and –475 mV were observed, which could be attributed to cytochromes and flavins (Wang et al., 2017), respectively. These results indicate that *S. onedensis* MR-1 could effectively utilize both direct and mediated electron transfer pathways with algal biochar anode. Okamoto et al. (2013) have shown that flavins secreted by *S. oneidensis* MR-1 improved the ability of cytochromes to transport electrons. The flavin/chtochromes interaction could facilitate redox reaction and regulate extracellular electron transport. Figure 3(d) shows that the CV profile for the graphite plate seemed like a cathode curve, which may caused by unknown cathode reaction occurred between electrode and solution under the condition of negative potential.

We also studied the adsorption of riboflavin (RF) by the electrode materials. When 5 mg of electrode materials were added into 100 μmol/L RF solution, the yellow color of the solution changed into colorless within a few minutes with algal biochar addition (Fig. 5(a)), whereas less RF was adsorbed by graphite powder, suggesting that algal biochar has excellent adsorption capacity for RF. The adsorption capacity was usually related to the surface area of materials (Tan et al., 2008). BET results show that the surface area of algal biochar (873 $m^2/g$) was significantly higher than that of graphite powder (25 $m^2/g$), suggesting better adsorption of RF by algal biochar than graphite powder.

To clarify if adsorption of redox mediator on biochar could enhance the EET of *S. onedensis* MR-1, sterile algal biochar electrode was immersed in 100 μmol/L RF solution for 24 h to adsorb RF. The algal biochar electrode with RF was used for electricity generation in BES. Our results showed that current production was improved three times using the biochar anode with RF adsorption (Fig. 5 (b)), suggesting that the adsorption of redox mediator by biochar could enhance the EET of *S. onedensis* MR-1. Wang et al. (2017) showed a similar report that graphene electrode with RF by spontaneous adsorption process exhibited higher power output than graphene electrode in microbial electrochemical systems.

Furthermore, electrochemical response of sterile electrodes to supplemented RF was studied using CV. The graphite plate and algal biochar electrodes were incubated in RF solution to reach equilibrium overnight. Then, the electrodes were scanned at 5 mV/s in mineral medium containing 5 μmol/L RF. As shown in Fig. 6, three pairs of redox peaks were obviously observed with algal biochar electrode. Compared with the CV profile without supplemented RF, the reductive peak at –478 mV and the oxidative peak at –421 mV could be attributed to the electrochemical redox reactions of riboflavin. The other two pairs may be ascribed to the redox substances in the

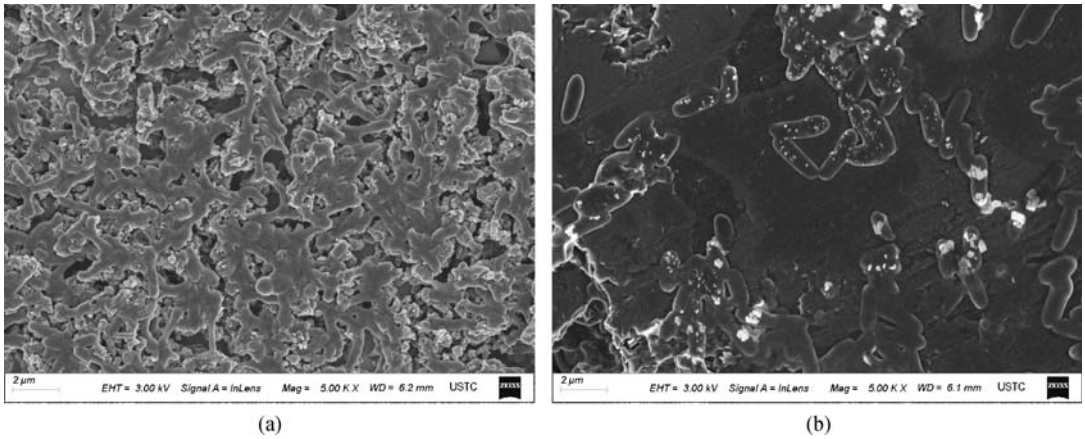


(a) (b)

**Fig. 4** SEM images of (a) algal biochar and (b) graphite plate anode when the current reached their maximum levels

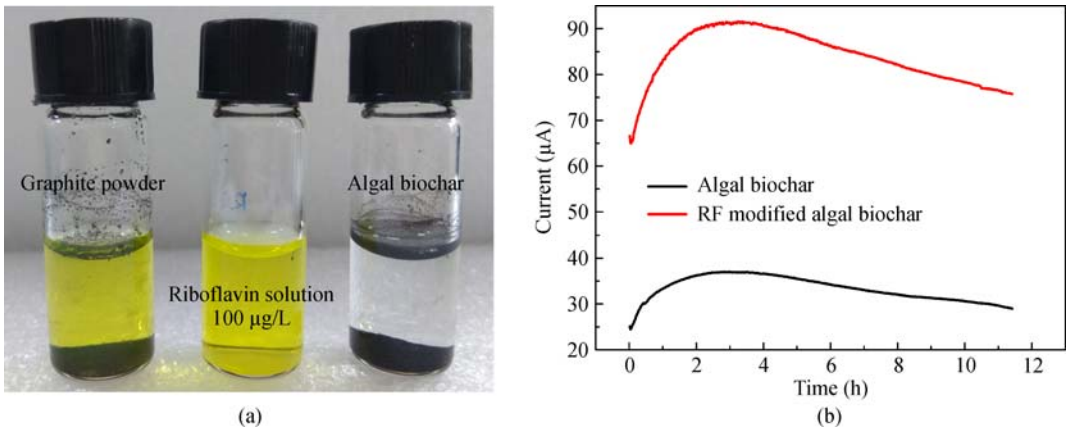


**Fig. 5** (a) Color changes of 100 μg/L riboflavin solution with 5 mg of graphite powder or algal biochar added; (b) Time course of current output with RF modified algal biochar anode

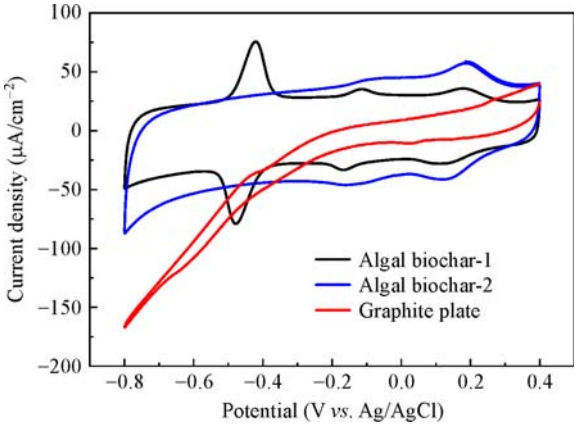


**Fig. 6** CV of riboflavin at sterile electrodes. Graphite plate and algal biochar-1 electrodes were in mineral medium containing 5 μmol/L riboflavin. Algal biochar-2 electrode was in mineral medium without riboflavin

mineral medium which could react on the electrode. No obvious or very weak peaks were detected with graphite plate electrodes under the same condition.

With the above results, it can be speculated that the greater biocurrent production with algal bloom derived biochar electrode could be accomplished in two ways. The algal biochar facilitates the attachment of bacterial cells onto the electrode surface, which contributes to direct electron transfer through the redox reactions between c-type cytochromes. On the other hand, the algal biochar exhibits excellent electrochemical response and adsorption capacity for redox mediator, which favors indirect electron transfer between riboflavin and electrodes.

## 4 Conclusions

In this study, we developed a novel bioanode using algal bloom derived biochar for efficient extracellular electron uptake in BESs. The algal biochar electrode could effectively utilize both indirect and direct electron transfer pathways for biocurrent generation. Compared with graphite plate electrode, the biochar electrode exhibits stronger electrochemical response and better adsorption for redox mediators. The BES with algal biochar anode showed greater performance in biocurrent generation ability than commercial graphite plate anode. This work provides an application potential for collected HAB to develop a cost-effective anode material for efficient extracellular electron uptake in bioelectrochemical systems, and to turn waste into resources.

**Acknowledgements** This work was supported by the National Natural Science Foundation of China (Grant Nos. 21477121 and 51538012) and the Fundamental Research Funds for the Central Universities.

## References

Alshehri A N Z (2017). Formation of electrically conductive bacterial nanowires by *Desulfuromonas acetoxidans* in microbial fuel cell reactor. International Journal of Current Microbiology and Applied Sciences, 6(8): 1197–1211

Avila A, Gregory B W, Niki K, Cotton T M (2000). An electrochemical approach to investigate gated electron transfer using a physiological model system: Cytochrome *c* immobilized on carboxylic acid-terminated alkanethiol self-assembled monolayers on gold electrodes. Journal of Physical Chemistry B, 104(12): 2759–2766

Bertaux J, Froehlich F, Ildefonse P (1998). Multicomponent analysis of FTIR spectra: Quantification of amorphous and crystallized mineral phases in synthetic and natural sediments. Journal of Sedimentary Research, 68(3): 440–447

Bian B, Shi D, Cai X B, Hu M J, Guo Q Q, Zhang C H, Wang Q, Sun A X L, Yang J (2018). 3D printed porous carbon anode for enhanced power generation in microbial fuel cell. Nano Energy, 44: 174–180

Chan K Y, Van Zwieten L, Meszaros I, Downie A, Joseph S (2008). Agronomic values of greenwaste biochar as a soil amendment. Soil

Research (Collingwood, Vic.), 45(8): 629–634

Chen Q, Pu W, Hou H, Hu J, Liu B, Li J, Cheng K, Huang L, Yuan X, Yang C, Yang J (2018a). Activated microporous-mesoporous carbon derived from chestnut shell as a sustainable anode material for high performance microbial fuel cells. Bioresource Technology, 249: 567–573

Chen S, Rotaru A E, Shrestha P M, Malvankar N S, Liu F, Fan W, Nevin K P, Lovley D R (2014). Promoting interspecies electron transfer with biochar. Scientific Reports, 4: 5019

Chen W W, Liu Z L, Hou J X, Zhou Y, Lou X G, Li Y X (2018b). Enhancing performance of microbial fuel cells by using novel double-layer-capacitor-materials modified anodes. International Journal of Hydrogen Energy, 43(3): 1816–1823

Creamer A E, Gao B, Zhang M (2014). Carbon dioxide capture using biochar produced from sugarcane bagasse and hickory wood. Chemical Engineering Journal, 249: 174–179

El Kasmi A, Wallace J M, Bowden E F, Binet S M, Linderman R J (1998). Controlling interfacial electron-transfer kinetics of cytochrome *c* with mixed self-assembled monolayers. Journal of the American Chemical Society, 120(1): 225–226

Fan Y, Xu S, Schaller R, Jiao J, Chaplen F, Liu H (2011). Nanoparticle decorated anodes for enhanced current generation in microbial electrochemical cells. Biosensors & Bioelectronics, 26(5): 1908–1912

Ferrari A C, Robertson J (2000). Interpretation of Raman spectra of disordered and amorphous carbon. Physical Review B: Condensed Matter and Materials Physics, 61(20): 14095–14107

Guo L (2007). Doing battle with the green monster of Taihu Lake. Science, 317(5842): 1166

Kashyap D, Dwivedi P K, Pandey J K, Kim Y H, Kim G M, Sharma A, Goel S (2014). Application of electrochemical impedance spectroscopy in bio-fuel cell characterization: A review. International Journal of Hydrogen Energy, 39(35): 20159–20170

Kim J R, Min B, Logan B E (2005). Evaluation of procedures to acclimate a microbial fuel cell for electricity production. Applied Microbiology and Biotechnology, 68(1): 23–30

Koposova E, Liu X, Kisner A, Ermolenko Y, Shumilova G, Offenhäusser A, Mourzina Y (2014). Bioelectrochemical systems with oleylamine-stabilized gold nanostructures and horseradish peroxidase for hydrogen peroxide sensor. Biosensors & Bioelectronics, 57: 54–58

Kotloski N J, Gralnick J A (2013). Flavin electron shuttles dominate extracellular electron transfer by *Shewanella oneidensis.* mBio, 4(1): e00553–12

Li S W, Zeng R J, Sheng G P (2017). An excellent anaerobic respiration mode for chitin degradation by *Shewanella oneidensis* MR-1 in microbial fuel cells. Biochemical Engineering Journal, 118: 20–24

Liu H, Matsuda S, Kato S, Hashimoto K, Nakanishi S (2010). Redox-responsive switching in bacterial respiratory pathways involving extracellular electron transfer. ChemSusChem, 3(11): 1253–1256

Liu N, Sun Z T, Wu Z C, Zhan X M, Zhang K, Zhao E F, Han X R (2013). Adsorption characteristics of ammonium nitrogen by biochar from diverse origins in water. Advanced Materials Research, 664: 305–312

Luo C H, Lü F, Shao L M, He P J (2015). Application of eco-compatible biochar in anaerobic digestion to relieve acid stress and promote the selective colonization of functional microbes. Water Research, 68: 710–718

Lv Q, Cao C B, Li C, Zhang J T, Zhu H X, Kong X, Duan X F (2003). Formation of crystalline carbon nitride powder by a mild solvothermal method. Journal of Materials Chemistry, 13(6): 1241–1243

Ma X X, Feng C H, Zhou W J, Yu H (2016). Municipal sludge-derived carbon anode with nitrogen-and oxygen-containing functional groups for high-performance microbial fuel cells. Journal of Power Sources, 307: 105–111

MacKintosh C, Beattie K A, Klumpp S, Cohen P, Codd G A (1990). Cyanobacterial microcystin-LR is a potent and specific inhibitor of protein phosphatases 1 and 2A from both mammals and higher plants. FEBS Letters, 264(2): 187–192

Meng X, Savage P E, Deng D (2015). Trash to treasure: From harmful algal blooms to high-performance electrodes for sodium-ion batteries. Environmental Science & Technology, 49(20): 12543–12550

Mohanakrishna G, Abu-Reesh I M, Al-Raoush R I, He Z (2018). Cylindrical graphite based microbial fuel cell for the treatment of industrial wastewaters and bioenergy generation. Bioresource Technology, 247: 753–758

Okamoto A, Hashimoto K, Nealson K H, Nakamura R (2013). Rate enhancement of bacterial extracellular electron transport involves bound flavin semiquinones. Proceedings of the National Academy of Sciences of the United States of America, 110(19): 7856–7861

Roberts D A, Paul N A, Cole A J, de Nys R (2015). From waste water treatment to land management: Conversion of aquatic biomass to biochar for soil amelioration and the fortification of crops with essential trace elements. Journal of Environmental Management, 157: 60–68

Sacco N J, Bonetto M C, Cortón E (2017). Isolation and characterization of a novel electrogenic bacterium, *Dietzia* sp. RNV-4. PLoS One, 12 (2): e0169955

Su Y, Li L, Hou J, Wu N, Lin W, Li G (2016). Life-cycle exposure to microcystin-LR interferes with the reproductive endocrine system of male zebrafish. Aquatic Toxicology (Amsterdam, Netherlands), 175: 205–212

Suguihiro T M, de Oliveira P R, de Rezende E I P, Mangrich A S, Marcolino Junior L H, Bergamini M F (2013). An electroanalytical approach for evaluation of biochar adsorption characteristics and its application for lead and cadmium determination. Bioresource Technology, 143: 40–45

Tan I A W, Ahmad A L, Hameed B H (2008). Adsorption of basic dye on high-surface-area activated carbon prepared from coconut husk: equilibrium, kinetic and thermodynamic studies. Journal of Hazardous Materials, 154(1–3): 337–346

ter Heijne A, Hamelers H V M, Saakes M, Buisman C J N (2008). Performance of non-porous graphite and titanium-based anodes in microbial fuel cells. Electrochimica Acta, 53(18): 5697–5703

Wang Q Q, Wu X Y, Yu Y Y, Sun D Z, Jia H H, Yong Y C (2017). Facile in-situ fabrication of graphene/riboflavin electrode for microbial fuel cells. Electrochimica Acta, 232: 439–444

Wu S, Fang G, Wang Y, Zheng Y, Wang C, Zhao F, Jaisi D P, Zhou D (2017). Redox-active oxygen-containing functional groups in activated carbon facilitate microbial reduction of ferrihydrite. Environmental Science & Technology, 51(17): 9709–9717

Xiao Y, Zheng Y, Wu S, Yang Z H, Zhao F (2016). Nitrogen recovery from wastewater using microbial fuel cells. Frontiers of Environmental Science & Engineering, 10(1): 185–191

Xing D, Cheng S, Logan B E, Regan J M (2010). Isolation of the exoelectrogenic denitrifying bacterium *Comamonas denitrificans* based on dilution to extinction. Applied Microbiology and Biotechnology, 85(5): 1575–1587

Xiong L, Chen J J, Huang Y X, Li W W, Xie J F, Yu H Q (2015). An oxygen reduction catalyst derived from a robust Pd-reducing bacterium. Nano Energy, 12: 33–42

Zhang F, Yuan S J, Li W W, Chen J J, Ko C C, Yu H Q (2015). $WO_3$ nanorods-modified carbon electrode for sustained electron uptake from *Shewanella oneidensis* MR-1 with suppressed biofilm formation. Electrochimica Acta, 152: 1–5

Zhang F, Yu S S, Li J, Li W W, Yu H Q (2016). Mechanisms behind the accelerated extracellular electron transfer in *Geobacter sulfurreducens* DL-1 by modifying gold electrode with self-assembled monolayers. Frontiers of Environmental Science & Engineering, 10 (3): 531–538

Zhang Y, Angelidaki I (2014). Microbial electrolysis cells turning to be versatile technology: Recent advances and future challenges. Water Research, 56: 11–25

Zhang Y Z, Mo G Q, Li X W, Zhang W D, Zhang J Q, Ye J S, Huang X D, Yu C Z (2011). A graphene modified anode to improve the performance of microbial fuel cells. Journal of Power Sources, 196 (13): 5402–5407

Zheng H, Guo W, Li S, Chen Y, Wu Q, Feng X, Yin R, Ho S H, Ren N, Chang J S (2017). Adsorption of p-nitrophenols (PNP) on microalgal biochar: Analysis of high adsorption capacity and mechanism. Bioresource Technology, 244(Pt 2): 1456–1464